ATL-PHYS-PROC-2023-043
20 July 2023

July 20, 2023

Probing the nature of electroweak symmetry breaking with Higgs boson pairs in ATLAS

Bartłomiej Żabiński
On behalf of the ATLAS Collaboration

The Henryk Niewodniczański
Institute of Nuclear Physics
Polish Academy of Sciences

Constraints on the Higgs boson trilinear self-coupling modifier κ_λ and non-SM HHVV coupling strength κ_{2V} are set by combining di-Higgs boson analyses using $b\bar{b}b\bar{b}$, $b\bar{b}\tau^+\tau^-$ and $b\bar{b}\gamma\gamma$ decay channels. The data used in these analyses were recorded by the ATLAS detector at the Large Hadron Collider in proton–proton collisions at $\sqrt{s} = 13$ TeV and corresponding to an integrated luminosity of 126–139 fb^{-1}. The combination of the di-Higgs analyses sets an upper limit of signal strength $\mu_{HH} < 2.4$ at 95% confidence level on the di-Higgs production and constraints for κ_λ between -0.6 and 6.6. The obtained confidence interval for κ_{2V} coupling modifier are [0.1,2.0] . The High Luminosity Large Hadron Collider prospects have been considered as well. The expected signal strength is 0.55 and κ_λ between 0.0 and 2.5 for the baseline scenario.

PRESENTED AT

DIS2023: XXX International Workshop on Deep-Inelastic Scattering and Related Subjects,
Michigan State University, USA, 27-31 March 2023

[1]

1 Introduction

The discovery of the Higgs boson by ATLAS [1] and CMS [2] experiments at the CERN Large Hadron Collider [3] opened opportunities to measure the boson's properties and test new hypotheses. In the Standard Model [4, 5, 6] Higgs boson potential [7, 8] provides spontaneous electroweak symmetry breaking that gives rise to its self-interactions. The Higgs boson self-interactions can be described among others by trilinear self-coupling λ_{HHH} that can be predicted at lowest order from Fermi constant G_F [9] and the Higgs mass m_H expressed by equation (1).

$$\lambda_{HHH} = \frac{m_H^2 G_F}{\sqrt{2}} \tag{1}$$

The validity of the SM in the Higgs sector can be tested using the 'kappa framework' [10, 11], in which a coupling modifier κ_m is defined as the ratio of the coupling strength between the particle m and Higgs boson to its SM value. The deviation of κ_m from unity would indicate physics processes beyond SM. For di-Higgs production κ_λ, κ_t, κ_V and κ_{2V} are considered. The κ_V and κ_t describe modifying the SM Higgs boson coupling to W or Z bosons and up-type quarks, respectively. The κ_{2V} is related to the VVHH interaction vertex. The κ_λ coupling modifiers can be measured in the gluon-gluon fusion process (ggF HH) and vector boson fusion (VBF). The κ_V and κ_{2V} can be measured in the VBF processes, κ_{2V} = 0 in the SM. At the LHC, Higgs boson pair-production is dominated by ggF processes and the overall cross-section in the SM is $\sigma^{SM}_{ggF}(pp \to HH) = 31.0^{+2.1}_{-7.2}$ fb at $\sqrt{s} = 13$ TeV [18]. The second largest Higgs pair-production process at LHC is VBF with $\sigma^{SM}_{VBF} = 1.72 \pm 0.04$ fb at $\sqrt{s} = 13$ TeV [12, 13]. Figure 1 represents leading order diagrams of the ggF and VBF production processes at the LHC featuring coupling modifiers described above.

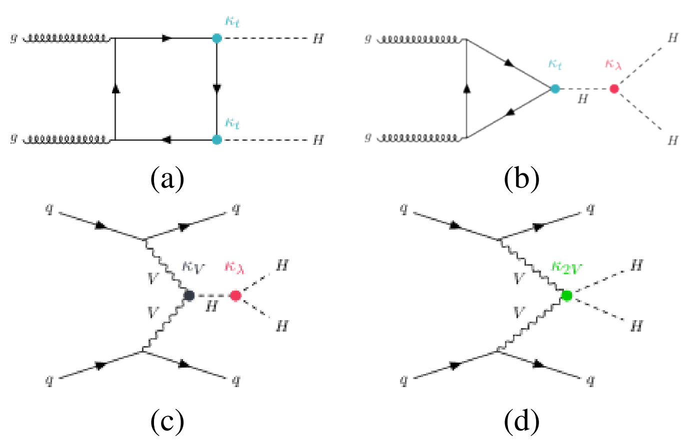

Figure 1: Examples of leading-order Feynman diagrams for Higgs boson pair production: for ggF production, diagram (a) is proportional to the square of the top-quark Yukawa coupling, while diagram (b) is proportional to the product of the top-quark Yukawa coupling and the Higgs boson self-coupling. For VBF production, diagram (c) and diagram (d) are proportional to the interactions κ_V and κ_{2V} between two vectors bosons and two Higgs bosons [17].

2 Higgs boson pair production in ATLAS

The Higgs pair-production is measured in different decay channels, but in this note, only the most sensitive channels $b\bar{b}b\bar{b}$, $b\bar{b}\gamma\gamma$ and $b\bar{b}\tau\tau$ [14, 15, 16] and their combination [17] will be discussed. Analysis-specific details can be found in the above-referenced publications. The first measured parameter of the combined results is signal strength μ_{HH} defined as a ratio of di-Higgs production cross-section including only ggF and VBF processes to its SM prediction of 32.7 fb [18, 19, 20]. The expected upper limit of μ_{HH} is 2.9. The observed upper limit in the absence of HH production, at 95% CL, is 2.4. The best-fit value obtained from the fit to the data μ_{HH}=-0.7 ± 1.3. is compatible with the SM prediction of unity, with p-value of 0.2. The obtained limits of μ_{HH} for each particular channel entering the combination and the results of the combination itself are shown in Figure 2 Figure 1.

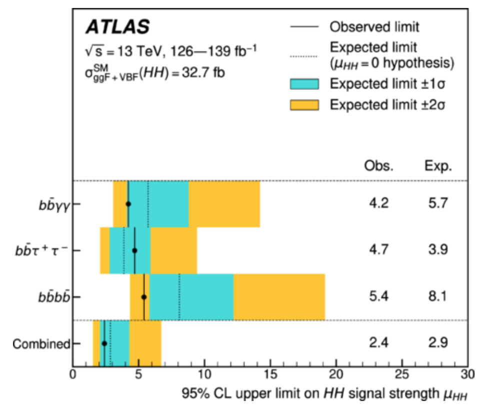

Figure 2: Observed and expected 95% CL upper limits on the signal strength for di-Higgs production from the $b\bar{b}b\bar{b}$, $b\bar{b}\tau^+\tau^-$ and $b\bar{b}\gamma\gamma$ decay channels, and their statistical combination. The value m_H = 125.09 GeV is assumed when deriving the predicted SM cross-section. The expected limit and the corresponding error bands are derived assuming the absence of the HH process and with all nuisance parameters profiled to the observed data [17].

The combination constraints for κ_λ and κ_{2V} coupling modifiers, related to $VVHH$ interaction vertex, are shown in Figure 3. Presented limits for κ_λ and κ_{2V} are obtained by using the values of the test statistic as a function of κ_λ in the asymptotic approximation and including the theoretical uncertainty of the cross-section predictions. The obtained confidence interval for κ_λ in each discussed analysis are collected in Table 1, and the combination constrain at 95% CL are -0.6 < κ_λ < 6.6 (observed) and -2.1 < κ_λ <7.8 (expected). The κ_{2V} coupling modifier for each mentioned channel and their combination have been obtained by fixing all other couplings modifiers to unity and with the expected value derived from the SM hypothesis. The expected and observed at 95% CL combined constraint for κ_{2V} are 0.0 < κ_{2V} < 2.1 and 0.1 < κ_{2V} < 2.0, respectively. Table 1 includes κ_{2V} constraints for each channel under combination.

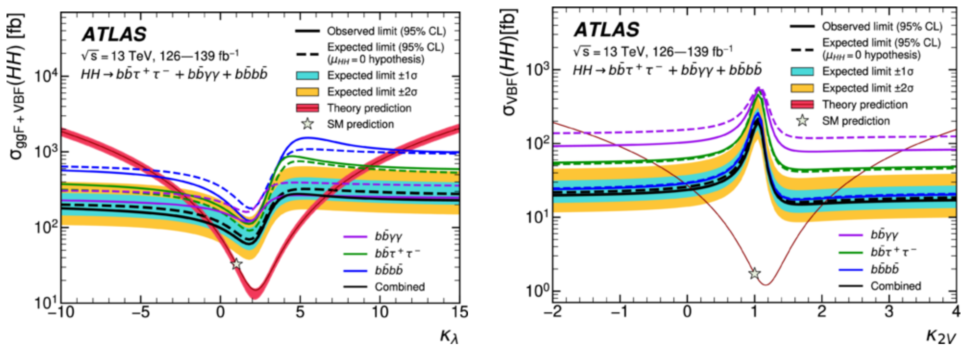

(a) (b)

Figure 3: Observed and expected 95% CL exclusion limits on the production cross-sections of (a) the combined ggF HH and VBF HH processes as a function of κ_λ and (b) the VBF HH process as a function of κ_{2V}, for the three di-Higgs search channels and their combination. The expected limits assume no HH production or no VBF HH production, respectively. The red line shows (a) the theory prediction for the combined ggF HH and VBF HH cross-section as a function of κ_λ where all parameters and couplings are set to their SM values except for κ_λ, and (b) the predicted VBF HH cross-section as a function of κ_{2V}. The bands surrounding the red cross-section lines indicate the theoretical uncertainty band in (b) is smaller than the width of the plotted line [17].

	$b\bar{b}b\bar{b}$	$b\bar{b}\tau\tau$	$b\bar{b}\gamma\gamma$	combination
Observed 95% CL	$-3.3 < \kappa_\lambda < 11.4$	$-2.7 < \kappa_\lambda < 9.5$	$-1.4 < \kappa_\lambda < 6.5$	$-0.6 < \kappa_\lambda < 6.6$
Expected 95% CL	$-5.2 < \kappa_\lambda < 11.6$	$-3.1 < \kappa_\lambda < 10.2$	$-3.2 < \kappa_\lambda < 8.1$	$-2.1 < \kappa_\lambda < 7.8$
Obs. value	$\kappa_\lambda = 6.2^{+3.0}_{-5.2}$	$\kappa_\lambda = 1.5^{+5.9}_{-2.5}$	$\kappa_\lambda = 2.8^{+2.0}_{-2.2}$	$\kappa_\lambda = 3.1^{+1.9}_{-2.0}$
Observed 95% CL	$0.0 < \kappa_{2V} < 2.1$	$-0.6 < \kappa_{2V} < 2.7$	$-0.8 < \kappa_{2V} < 3.0$	$0.1 < \kappa_{2V} < 2.0$
Expected 95% CL	$-0.0 < \kappa_{2V} < 2.1$	$-0.5 < \kappa_{2V} < 2.7$	$-1.6 < \kappa_{2V} < 3.7$	$0.0 < \kappa_{2V} < 2.1$
Obs. value	$\kappa_{2V} = 1.0^{+0.7}_{-0.6}$	$\kappa_{2V} = 1.5^{+0.7}_{-1.7}$	$\kappa_{2V} = 1.1^{+1.0}_{-1.0}$	$\kappa_{2V} = 1.1^{+0.6}_{-0.6}$

Table 1: Summary of κ_λ and κ_{2V} observed and expected constraints and corresponding observed best-fit values with their uncertainties for the $HH \to b\bar{b}b\bar{b}$, $HH \to b\bar{b}\tau\tau$, $HH \to b\bar{b}\gamma\gamma$, analyses and for the di-Higgs combination. Limits are obtained using the test statistic (-2 lnΛ) in the asymptotic approximation. The expected constraints are derived under the SM assumption. All other coupling modifiers are fixed to the SM value.

3 Prospects of double Higgs production at the HL-LHC

The High Luminosity LHC (HL-LHC) is expected to start in 2029. During the HL-LHC operation it is expected to obtain a total integrated luminosity of 3000 fb^{-1} at a center of mass energy $\sqrt{s}$ = 14 TeV. The expected total number of the collected data is significantly larger than the collected data during the LHC Run-2 offers great conditions to measure the Higgs trilinear self-coupling. The prospects of the di-Higgs production at HL-LHC were obtained by scaling full Run-2 distributions and considering multiple scenarios of systematic uncertainties [21]. The scale factors are applied to take into account the integrated luminosity and increase of center-of-mass energy. Four cases of future uncertainties are considered:

- Only statistical uncertainties are considered (No syst. unc).
- A baseline scenario where the relevant systematic uncertainties were scaled down with respect to expected HL-LHC data delivered [22]. The data-driven background uncertainties are also reduced according to the integrated luminosity. This relies on a 50% reduction of the bootstrap uncertainty at the HL-LHC, while the shape uncertainty is assumed to be identical to Run-2.
- A scenario where experimental uncertainties from Run-2 are unchanged and theoretical uncertainties associated with HH signal are halved (Theoretical unc. halved).
- The experimental uncertainties from Run-2 are left unchanged (Run-2 syst. unc).

Figure 4 represents the result of the prospect studies. The signal strength for the baseline scenario at 95% CL is 0.55. The constraint on κ_λ in the same scenario is within the range from 0.0 to 2.5. The results for the rest of the scenarios and more details about discussed prospects are in the note [21].

4 Conclusions

The double Higgs production searches offer a unique opportunity to investigate the mechanism of electroweak symmetry-breaking. The measurement of λ_{HHH} is challenging due to very small cross-sections of the di-Higgs production processes. Constraints are set on the signal strength μ as well as on κ_λ and κ_{2V}. Obtained limits scope for each considered channel are wide, but by the combination of all channels, the constraints have been limited to $0.1 < \kappa_{2V} < 2.0$ and $-0.6 < \kappa_\lambda < 6.6$. The di-Higgs searches are also a good probe for beyond Standard Model heavy resonance searches [23, 24, 25]. The ATLAS experiment is in the Run-3 phase, where it is expected to collect two times more data than during Run-2 and finally reach LHC runs with high luminosity. That significant amount of data will offer spectacular results in the mentioned channels and even more, so please stay tuned.

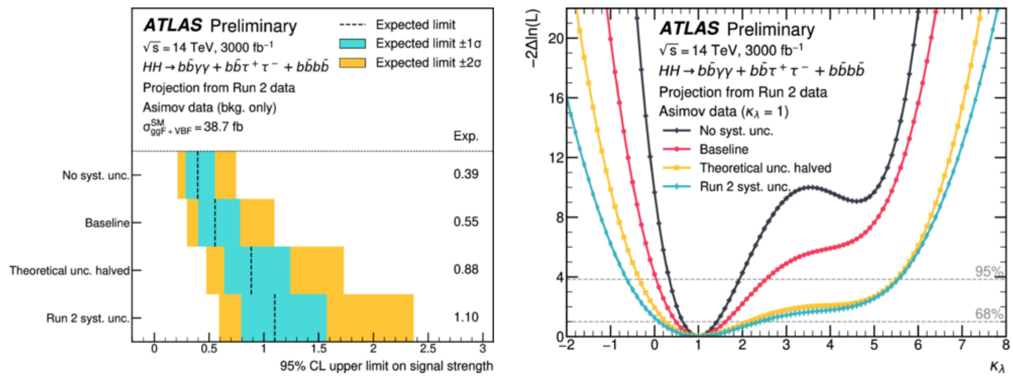

(a) (b)

Figure 4: Projected 95% CL upper limits on the signal strength (a) and negative log-profile-likelihood as a function of κ_λ evaluated on Asimov datasets constructed under the SM hypothesis of $\kappa_\lambda = 1$ (b), combining the $b\bar{b}b\bar{b}$, $b\bar{b}\gamma\gamma$ and $b\bar{b}\tau\tau$ channels at 3000 fb^{-1} and $\sqrt{s}$ = 14 TeV for four uncertainty scenarios described in the text. The limits are derived assuming no HH production.

Funding informaion This work is supported in part by the Polish Ministry of Education and Science project no. 2022/WK/08.

References

[1] ATLAS Collaboration, *Observation of a new particle in the search for the Standard Model Higgs boson with the ATLAS detector at the LHC*, Physics Letters B **716** (2012) 1, arXiv:1207.7214 [hep-ex]

[2] CMS Collaboration, *Observation of a new boson at a mass of 125 GeV with the CMS experiment at the LHC*, Physics Letters B **716** (2012) 30, arXiv:1207.7235

[3] L. Evans, P. Bryant (Eds.), *LHC Machine*, JINST 3 (2008) S08001.

[4] S.L. Glashow, *Partial-symmetries of weak interactions*, Nucl. Phys. **22** (1961) 579.

[5] A.Salam, *Weak and Electromagnetic Interactions*, Conf. Proc. C**680519** (1968). Proceedings of the eight Nobel sumphosium.

[6] S.Weinberg, *A model of leptons*, Phys. Rev. Lett. **19** (1967) 1264.

[7] F.Englert and R.Brout, *Broken Symmetry and the Mass of Gauge Vector Mesons*, Phys. Rev. Lett **13** (1964) 321.

[8] P.W.Higgs, *Broken symmetries, massles particles and gauge fields*, Phys. Rev. Lett. **12** (1964) 132.

[9] Particle Data Group, R.L. Workman et al. *Review of Particle Physics*, PTEP **2022** (2022) 083C01.

[10] LHC Higgs Cross Section Working Group, S. Heinemeyer et al., *Handbook of LHC Higgs Cross Sections:3. Higgs Properties*, CERN-2013-004 (CERN,Geneva,2013), arXiv:1307.1347 [hep-ph].

[11] LHC Higgs Cross Section Working Group, D. de Florian et al., *Handbook of LHC Higgs Cross Sections:4. Description of Nature of the Higgs Sector*, CERN-2017-002-M (CERN,Geneva,2017), arXiv:1610.07922 [hep-ph].

[12] R. Frederix, S. Frixione, V. Hirschi, F. Maltoni, O. Mattelaer, P. Torrielli, E. Vryonidou, and M. Zaro, *Higgs pair production at the LHC with NLO and parton-shower effects*, Phys. Lett. B **732** (2014) 142, arXiv:1401.7340

[13] Frédéric A. Dreyer, Alexander Karlberg, *Fully differential Vector-Boson Fusion Higgs Pair Production at Next-to-Next-to-Leading Order*, Phys. Rev. D **99**, 074028 (2019), arXiv:1811.07918 [hep-ph]

[14] ATLAS Collaboration, *Search for nonresonant pair production of Higgs bosons in the $b\bar{b}b\bar{b}$ final state in pp collisions at $\sqrt{s} = 13$ TeV with the ATLAS detector*, CERN-EP-2022-235, arXiv:2301.03212 [hep-ex]

[15] ATLAS Collaboration, *Search for Higgs boson pair production in the two bottom quarks plus two photons final state in pp collisions at* $\sqrt{s} = 13$TeV *with the ATLAS detector*, Phys. Rev. D, **106** (2022) 052001, arXiv:2112.11876 [hep-ex]

[16] ATLAS Collaboration, *Search for resonant and non-resonant Higgs boson pair production in the $b\bar{b}\tau^+\tau^-$ decay channel using 13 TeV pp collision data from the ATLAS detector*, CERN-EP-2022-109, arXiv:2209.10910 [hep-ex]

[17] ATLAS Collaboration, *Constraints on the Higgs boson self-coupling from single- and double-Higgs production with the ATLAS detector using pp collisions at $\sqrt{}$=13 TeV*, Phys. Lett. B, **843** (2023) 137745, arXiv:2211.01216 [hep-ex]

[18] M. Grazzini et al., *Higgs boson pair production at NNLO with top quark mass effects*, JHEP 05 (2018) 059, arXiv: 1803.02463 [hep-ph].

[19] G. Heinrich, S. P. Jones, M. Kerner, G. Luisoni and L. Scyboz, *Probing the trilinear Higgs boson coupling in di-Higgs production at NLO QCD including parton shower effects*, JHEP 06 (2019) 066, arXiv: 1903.08137 [hep-ph].

[20] D. de Florian and J. Mazzitelli, *Higgs Boson Pair Production at Next-to-Next-to-Leading Order in QCD*, Phys. Rev. Lett. **111** (2013) 201801, arXiv: 1309.6594 [hep-ph].

[21] ATLAS Collaboration, *HL-LHC prospects for the measurement of Higgs boson pair production in the $b\bar{b}b\bar{b}$ final state and combination with the $b\bar{b}\gamma\gamma$ and $b\bar{b}\tau\tau$ final states at the ATLAS experiment*, ATL-PHYS-PUB-2022-053

[22] A. Dainese et al., *Report on the Physics at the HL-LHC, and Perspectives for the HE-LHC*, CERN Yellow Report CERN-2019-007, 2019, url: https://cds.cern.ch/record/2703572 (cit. on pp. 2, 6).

[23] ATLAS Collaboration, *Search for Higgs boson pair production in the two bottom quarks plus two photons final state in pp collisions at $\sqrt(s)$=13 TeV with the ATLAS detector*, Phys. Rev. D **106** (2022) 052001, arXiv:2112.11876 [hep-ex].

[24] ATLAS Collaboration, *Reconstruction and identification of boosted di$-\tau$ systems in a search for Higgs boson pairs using 13 TeV proton-proton collision data in ATLAS*, JHEP 11 (2020) 163, arXiv:2007.14811 [hep-ex].

[25] ATLAS Collaboration, *Search for resonant pair production of Higgs bosons in the $b\bar{b}b\bar{b}$ final state using pp collisions at $\sqrt(s)$ = 13 TeV with the ATLAS detector*, Phys. Rev. D **105** (2022) 092002, arXiv:2202.07288 [hep-ex].